Structure-Based Analysis of the β8 Interactive Sequence of Human αB Crystallin†

Joy G. Ghosh,‡,§ Marcus R. Estrada,§ and John I. Clark*,‡,§,||

Biomolecular Structure and Design, Department of Biological Structure, and Department of Ophthalmology, University of Washington, Seattle, Washington 98195-7420

Received May 16, 2006; Revised Manuscript Received June 20, 2006

ABSTRACT: The functional importance of the β8 sequence ($_{131}$LTITSSLS$_{138}$), which is on the surface of the α crystallin core domain of human αB crystallin, was evaluated using site-directed mutagenesis. Ultraviolet circular dichroism determined that mutating the surface-exposed, nonconserved residues, Leu-131, Thr-132, Thr-134, Ser-135, Ser-136, and Ser-138 individually or in combination (αAβ8 and CEβ8), had no measurable effect on secondary and tertiary structure. Size exclusion chromatography determined the size of the complexes formed by the β8 mutants to be 6−8 subunits larger than wt αB crystallin. In chaperone assays, the protective effect of the L131S, T132A, and S135C mutants of the β8 sequence was similar to wt αB crystallin when β_L crystallin and alcohol dehydrogenase were the chaperone substrates and decreased to 66% when citrate synthase was the chaperone substrate. In contrast, the chaperone activity for all three substrates was dramatically reduced for the T134K, S138A, S136H, and CEβ8 mutants. The prominent location of Thr-134, Ser-136, and Ser-138 on the exposed surface of the α crystallin core domain could account for the effect on complex assembly and chaperone activity. Modulation of chaperone activity by the exposed residues of the β8 sequence in the α crystallin core domain was independent of complex size. The results established the β3−β8−β9 surface of the α crystallin core domain as an interface for complex assembly and chaperone activity.

Small heat shock proteins (sHSP)[1] are proteins with molecular masses <43 kDa that respond to stress in lens, brain, skin, kidney, and muscle to recognize, stabilize, and protect unfolding proteins from aggregation and insolubilization (*1*−*14*). The common structural feature of sHSPs is an immunoglobulin-like domain called the α crystallin core domain which consists of six to ten β strands arranged in two antiparallel β sheets to form a compact β sandwich (*15*−*23*). Electron spin resonance and homology modeling of αB crystallin indicated that β strands 2, 3, 8, and 9 formed one β sheet and β strands 4, 5, and 7 formed the facing antiparallel β sheet of the α crystallin core domain (*15*, *17*, *24*−*26*). Of the seven interactive sequences identified previously using protein pin arrays, three interactive sequences, β3, β8, and β9, formed an interface on the surface of the α crystallin core domain indicating potential involvement in chaperone function and complex assembly (*24*, *25*). Mutational analysis established that the surface-exposed side chains of the β3 and β9 strands were important for the recognition and selection of substrate proteins on the basis of the amount of substrate protein unfolding (*19*, *27*). Novel fluorescence resonance energy transfer, mass spectrometry, and size exclusion chromatography characterized the β4−β8 groove on the surface of the α crystallin core domain of human αB crystallin as an ATP interactive site and established a relationship between enhanced chaperone activity and altered subunit dynamics in the presence of ATP.

While the importance of the conserved α crystallin core domain in chaperone activity is well established (*16*, *18*, *19*, *28*−*39*), three sHSPs, 12.2, 12.3, and 12.6 from *Caenorhabditis elegans* (*C. elegans*) that contain the α crystallin core domain, lack chaperone activity in vitro (*40*). Replacing the N- and C-terminal domains of *C. elegans* sHSP12.2 with the N- and C-terminal domains of αB crystallin failed to restore chaperone activity even though the resultant N-c-T chimera formed assemblies similar to αB crystallin (*41*). These results suggested that differences in the primary sequence of the interactive sequences in the α crystallin core domain may be responsible for differences in function. Mutational analysis of the β3 sequence of αB crystallin performed on the basis of the differences in the amino acid composition of the β3 sequences of αB crystallin, αA crystallin, and *C. elegans* sHSP12.2 confirmed the hypothesis that differences in the amino acid composition of interactive sequences in the α crystallin core domain of sHSPs accounted for differences in chaperone activity (*27*). The results were consistent with the theory that chaperone activity was dependent on the composition of the interactive sequences in the α crystallin core domain and independent of complex size.

The current study evaluated the effect of mutating selected residues in the β8 sequence of human αB crystallin on the basis of sequence differences between the β8 sequences of human αB crystallin, human αA crystallin, and *C. elegans*

† Supported by Grant EY04542 from the National Eye Institute.

* To whom correspondence should be addressed at the Department of Biological Structure, HSB G514, Box 357420, University of Washington. Phone: 206-685-0950. Fax: 206-543-1524. E-mail: clarkji@u.washington.edu.

‡ Biomolecular Structure and Design, University of Washington.

§ Department of Biological Structure, University of Washington.

|| Department of Ophthalmology, University of Washington.

[1] Abbreviations: sHSP, small heat shock protein; MOE, molecular operating environment; UVCD, ultraviolet circular dichroism; ADH, alcohol dehydrogenase; CS, citrate synthase.

10.1021/bi060970k CCC: $33.50
Published on Web 07/25/2006

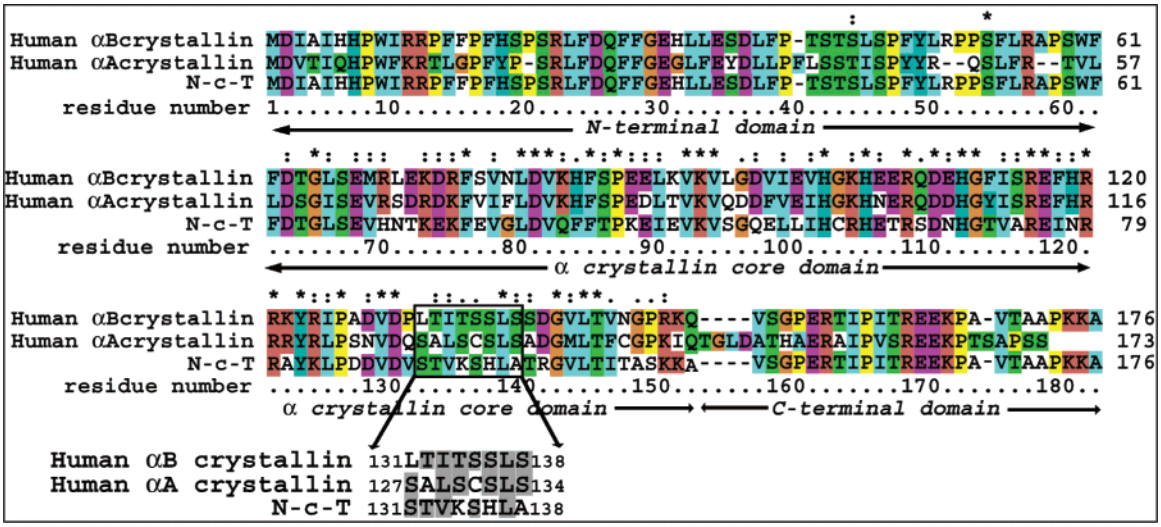

FIGURE 1: ClustalX-generated sequence alignment of human αB crystallin, human αA crystallin, and the N-c-T chimera of *C. elegans* sHSP12.2 and αB crystallin that lacks chaperone activity in vitro (*41*). The β8 sequences in the three proteins were identified (box) and expanded at the bottom of the figure. Conserved residues have gray backgrounds. The L131S substitution was common to both αA crystallin and the N-c-T chimera. Residues Thr-132 and Ser-135 in human αB crystallin were substituted with corresponding residues Ala-128 and Cys-131 from human αA crystallin. Residues Thr-134, Ser-136, and Ser-138 in αB crystallin were substituted with corresponding residues Lys-93, His-95, and Ala-97 from the N-c-T chimera. Conserved residues were designated by "*" or ":" in their column headings, where "*" represented identical amino acids and ":" represented chemically similar amino acids.

Table 1: Primers Used for Site-Directed Mutagenesis of the β8 Strand of αB Crystallin[a]

mutation	type	primer sequence (5′ → 3′)
L131S	forward	CCA GCT GAT GTA GAC CCT **TCG** ACC ATC ACT TCA TCC CTG TCA TCC
	reverse	GGA TGA AGT AAT GGT CGA AGG GTC TAC ATC
T132A	forward	CT GAT GTA GAC CCT CTC **GCA** ATT ACT TCA TCC CTG TCA TCT G
	reverse	C AGA TGA CAG GGA TGA AGT AAT TGC GAG AGG GTC TAC ATC AG
T134K	forward	GTA GAC GAC CCT CTC ACC ATC **AAG** TCA TCC CTG TCA TCT GAT GGG
	reverse	AGA TGA TAA GGA TGA CTT AAT GGT GAG AGG GTC
S135C	forward	GAC CCT CTC ACC ATT ACT **TGC** TCC CTG TCA TCT GAT GGG GTC
	reverse	GAC CCC ATC AGA TGA CAG GGA GCA AGT AAT GGT GAG AGG GTC
S136H	forward	GAC CCT CTC ACC ATT ACT TCA **CAT** CTG TCA TCC GAT GGG GTC CTC
	reverse	GGA TCC ATC AGA TGA CAA ATG TGA AGT AAT GGT GAG
S138A	forward	CTC ACC ATT ACT TCA TCC CTG **GCA** TCT GAC GGG GTC CTC ACT GTG
	reverse	AGA GAC TCC GTC AGA TGC TAA AGA TGA AGT AAT GGT
αAβ8	forward	CAC AGT GAG GAC CCC ATC **GGC TGA CAG GGA GCA GGA GAG GGC TGA** AGG GTC TAC ATC AGC TGG
	reverse	CCA GCT GAT GTA GAC CCT **TCA GCC CTC TCC TGC TCC CTG TCA GCC** GAT GGG GTC CTC ACT GTG
CEβ8	forward	CAC AGT GAG GAC CCC ATC **CCT AGT GGC CAG GTG TGA CTT TAC GGT GGA** AGG GTC TAC ATC AGC TGG
	reverse	CCA GCT GAT GTA GAC CCT **TCC ACC GTA AAG TCA CAC CTG GCC ACT AGG** GAT GGG GTC CTC ACT GTG

[a] Column 1 lists the substitutions, column 2 lists the type of primer (forward or reverse), and column 3 lists the nucleotide sequence of the primer used with the actual substitutions in bold face.

sHSP12.2. Six single-site mutants, L131S, T132A, T134K, S135C, S136H, and S138A, and two multisite chimeric mutants, αAβ8 and CEβ8, of the β8 motif of αB crystallin were constructed and synthesized on the basis of a comparison of the primary sequence and predicted secondary structure of αB crystallin, αA crystallin, and *C. elegans* sHSP12.2. The β8 mutants assembled into complexes that were 6−8 subunits larger than wt αB crystallin. The effect of the mutations on chaperone activity was dramatic in the absence of measurable structural modifications evaluated using ultraviolet circular dichroism (UVCD) and size exclusion chromatography. The results established the functional importance of the exposed residues of the β8 interactive sequence in the chaperone activity and complex assembly of αB crystallin, the archetype of sHSPs.

EXPERIMENTAL PROCEDURES

Multiple Sequence Alignment and Rationale for Mutagenesis. Nonconserved, surface-exposed residues of the β8 motif, $_{131}$**LT**I**TSS**L**S**$_{138}$, of human αB crystallin were substituted on the basis of a sequence alignment of αB crystallin and αA crystallin, two sHSPs with chaperone-like activity in vitro and the N-c-T chimera, a sHSP with no chaperone-like activity in vitro (*41*) (Figure 1). The *C. elegans* sHSP12.2 and human αB crystallin chimera (N-c-T) contains the α crystallin core domain of *C. elegans* sHSP12.2 and the N- and C-termini of αB crystallin. Secondary structure information from the homology models of human αA crystallin and αB crystallin computed using the wheat sHSP16.9 crystal structure and predicted secondary structure information of the N-c-T chimera were incorporated into the alignment (*24*, *25*). The L131S mutation was common to both αA crystallin and the N-c-T chimera. The αA crystallin based single-site β8 substitutions were T132A and S135C. The N-c-T chimera based single-site β8 substitutions were T134K, S136H, and S138A. In addition, the entire β8 motif of αB crystallin, $_{131}$LTITSSLS$_{138}$, was replaced with the β8 motif, $_{127}$SALSC-

SLS_{134}, from αA crystallin (αAβ8) and the β8 motif, $_{90}$STVKSHLA$_{97}$, from the N-c-T chimera (CEβ8) (Figure 1). Residues 133 and 137 of αB crystallin formed intramolecular contacts (*24*), were chemically similar or identical to residues at the corresponding positions in the β8 motifs of αA crystallin and the N-c-T chimera, and were consequently not mutated. Eight substitutions were made to the β8 motif of αB crystallin, and the resultant mutants are referred to as "β8 mutants" in the remainder of the paper.

Mutagenesis, Protein Expression, and Purification. Site-directed mutagenesis of the β8 motif of αB crystallin was performed using the QuikChange site-directed mutagenesis kit (Stratagene, La Jolla, CA) and custom primers (Qiagen, Valencia, CA) (Table 1) as described previously (*27*). Wt αB crystallin and the β8 mutants were purified using methods described previously with minor modifications (*19*, *27*). Protein concentrations were determined using the BCA protein assay kit (Pierce, Rockford, IL). Proteins were dialyzed into 5 mM PBS, pH 7.0, and stored at −80 °C for further analysis.

Circular Dichroism. Subtle changes in 3-D structure cannot be ruled out by UVCD spectroscopic analysis, and the inherent polydispersity of αB crystallin prevented a more thorough structural analysis of the β8 mutants using X-ray diffraction or NMR spectroscopy. The secondary and tertiary structures of wt αB crystallin and the eight β8 mutants were determined by ultraviolet circular dichroism using a Jasco 720 circular dichroism spectrophotometer at 37 and 50 °C as described previously (*27*). Far-UVCD experiments were performed using samples at a concentration of 0.1 mg/mL in 5 mM PBS, pH 7.0, with a 1 mm path length cuvette, while near-UVCD experiments were performed with samples that were at 5 mg/mL concentration in 5 mM PBS, pH 7.0, with a 1 mm path length cuvette. Five spectra were collected for each sample at each temperature. The near- and far-UVCD spectra of the buffer (5 mM PBS, pH 7.0) were used for baseline correction. Raw UVCD ellipticities were converted to mean residue molar ellipticities and expressed as deg·cm^2·dmol^{-1} to normalize for slight molecular mass differences between wt αB crystallin and the β8 mutants.

Size Exclusion Chromatography. The complex size of wt αB crystallin and the eight β8 mutants was determined using a Biosep SEC-S4000 column with a molecular mass range of 15−2000 kDa (Phenomenex, Torrance, CA) and an AKTA FPLC purifier (Amersham Biosciences, Piscataway, NJ) as described previously (*27*). In three separate runs, 30 μL samples (2.5 mg/mL) were loaded on a preequilibrated column and chromatographed at a flow rate of 1.0 mL/min in 5 mM PBS, pH 7.0. The apparent molecular mass and the average number of subunits per complex formed by wt αB crystallin and the β8 mutants were calculated from a plot of the elution time versus log(apparent molecular mass) of the calibration proteins as described previously (*27*). Polydispersity of the elution peaks was calculated as peak width at half peak height.

Chaperone Assays. Chaperone assays with wt αB crystallin and the eight β8 mutants were performed using previously established methods with minor modifications (*19*, *27*). Chaperone assays were performed at concentrations that permit detection of small changes in the chaperone activity of the β8 mutants. Initially, chaperone assays were performed at a 10:1, 5:1, 1:1, 1:5, and 1:10 ratio of chaperone:substrate to determine optimal conditions. A 1:1 monomeric molar ratio of chaperone:substrate was determined to be the optimum ratio. All subsequent chaperone assays of the β8 mutants were performed in triplicate and at a 1:1 monomeric molar ratio of chaperone:substrate protein. The chaperone activity of wt αB crystallin and all eight β8 mutants was conducted simultaneously with bovine β_L crystallin (25 kDa) (Sigma, St. Loius, MO), equine alcohol dehydrogenase (ADH) (40 kDa) (Sigma, St. Loius, MO), and porcine citrate synthase (CS) (47 kDa) (Roche, Indianapolis, IN) in a 96-well ELISA microtiter plate. In each well, 0.1 mmol of the chaperone and substrate was mixed in a total volume of 200 μL buffer (5 mM PBS, pH 7.0). Light scattering at $\lambda = 340$ nm was measured using a Multiskan MCC/340 plate reader before heating (time = 0). After the first reading, the plate was heated at 50 °C, and readings were taken at 15 min intervals for 60 min. Chaperone activity was calculated as aggregation and percentage protection in which the maximum light scattering of each substrate protein in the absence of any chaperone was set as 0% protection (Table 3).

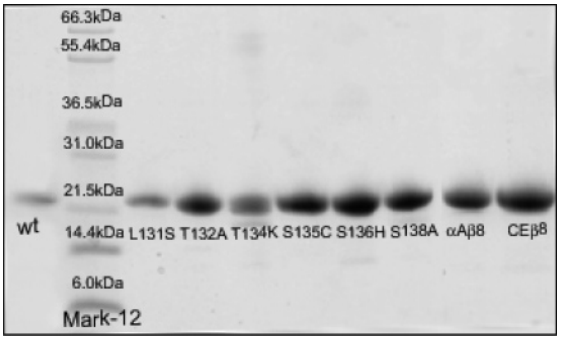

FIGURE 2: SDS−PAGE analysis of purified wt αB crystallin and eight β8 mutants. Lane 1 contains the purified wt αB crystallin. Lane 2 contains the molecular mass standards. Lanes 3−10 contain purified αB crystallin mutants L131S, T132A, T134K, S135C, S136H, S138A, αAβ8, and CEβ8, respectively. Wt αB crystallin and the eight β8 mutants were >97% pure as determined by SDS−PAGE analysis.

Molecular Modeling. The three-dimensional homology model of human αB crystallin was computed using the X-ray crystal structure of wheat sHSP16.9 as the template as described previously (*21*, *24*, *27*). The Cα root mean square deviation between the superimposed model of human αB crystallin and the crystal structure of wheat sHSP16.9 was 3.25 Å.

RESULTS

Six αB crystallin single-site β8 mutants, L131S, T132A, T134K, S135C, S136H, and S138A, and two chimeric β8 mutants, αAβ8 and CEβ8, were designed and synthesized on the basis of differences in the primary amino acid sequences of αB crystallin, αA crystallin, and the N-c-T chimera of αB crystallin and *C. elegans* sHSP12.2 (Figure 1). The αAβ8 and CEβ8 mutants are αB crystallin chimeric mutants in which the entire β8 sequence ($_{131}$LTITSSLS$_{138}$) of wt αB crystallin was swapped with the β8 sequences of αA crystallin ($_{127}$SALSCSLS$_{134}$) and the N-c-T chimera ($_{131}$STVKSHLA$_{138}$), respectively. Wt αB crystallin and the eight β8 mutants were expressed and purified to apparent homogeneity using ion-exchange and size exclusion chromatography (see Experimental Procedures). SDS−PAGE and

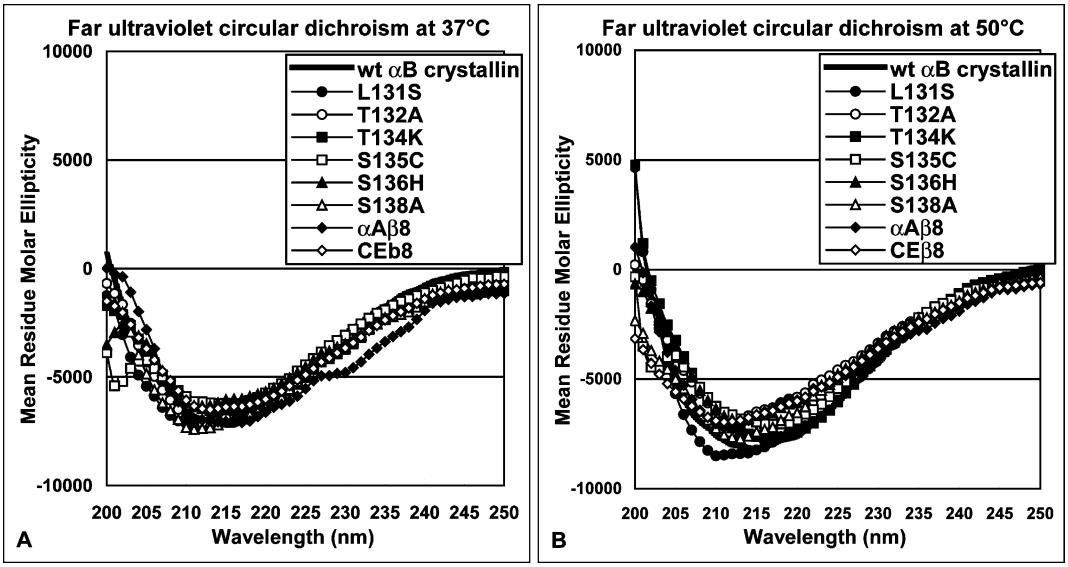

FIGURE 3: Far-UVCD of wt αB crystallin and the eight β8 mutants. For each protein, the average of five spectra acquired at 37 °C (A) and 50 °C (B) between 200 and 250 nm was plotted. The UVCD signal was converted to mean residue molar ellipticity expressed as deg·cm^2·dmol^{-1} to normalize for slight differences in molecular mass between wt αB crystallin and the mutants. At each temperature, the UVCD spectrum of wt αB crystallin contained a single broad minimum between 207 and 217 nm. The UVCD spectra of the β8 mutants were similar in shape to the UVCD spectra of wild-type αB crystallin and had negative ellipticities at the same minima.

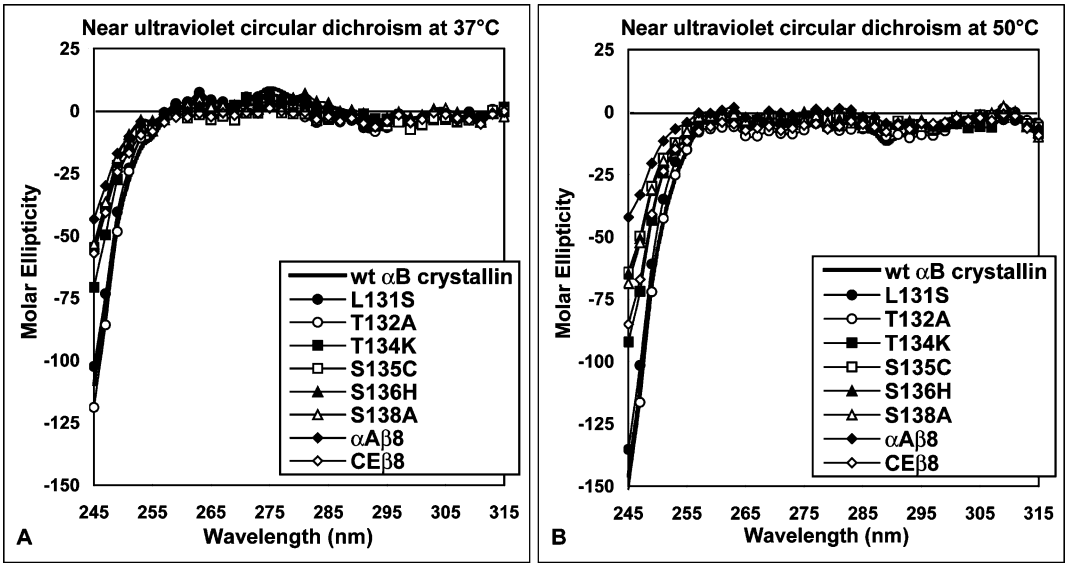

FIGURE 4: Near-UVCD of wt αB crystallin and the eight β8 mutants. For each protein, the average of five spectra acquired at 37 °C (A) and 50 °C (B) between 245 and 315 nm was plotted. The UVCD signal was converted to molar ellipticity expressed in deg·cm^2·dmol^{-1} to normalize for slight differences in molecular mass between wt αB crystallin and the mutants. The spectra for the β8 mutants resembled the spectrum for wt αB crystallin at 37 and 50 °C (molar ellipticity [Θ]: 37 °C > 50 °C). Mutations in the β8 motif of αB crystallin did not appear to alter the tertiary structure of αB crystallin.

densitometric analysis determined the purity of the mutants to be >97% (Figure 2).

The effect of the β8 mutations on the secondary structure of αB crystallin was determined by far-UVCD at 37 and 50 °C (Figure 3). Wt αB crystallin had a single broad minimum between 207 and 217 nm at 37 and 50 °C, which represented a structure rich in β sheet and β turn with little helical content, which was consistent with previous reports of the far-UVCD and electron spin resonance spectra for wt αB crystallin. A small decrease in ellipticity between 200 and 205 nm was observed in the spectrum of the S135C mutant, which was not observed in the far-UVCD spectra of the other αB crystallins. The far-UVCD spectra of all eight β8 mutants resembled wt αB crystallin at both 37 and 50 °C, which indicated that substituting residues in the β8 motif of αB crystallin had no measurable effect on the β sheet rich secondary structure of wt αB crystallin.

The effect of the β8 mutations on the tertiary structure of αB crystallin was determined by near-UVCD at 37 and 50 °C (Figure 4). The near-UVCD spectra of wt αB crystallin and the eight β8 mutants were similar and contained positive absorption peaks at 260 and 267 nm for phenylalanine, at 277 nm for tyrosine, and at 285 nm for tryptophan. Mutations in the β8 motif had no measurable effect on the tertiary structure of human αB crystallin. The magnitude of the absorption peaks in the spectra of wt αB crystallin and all eight β8 mutants responded in the same way as the temperature was increased from 37 to 50 °C. The near- and

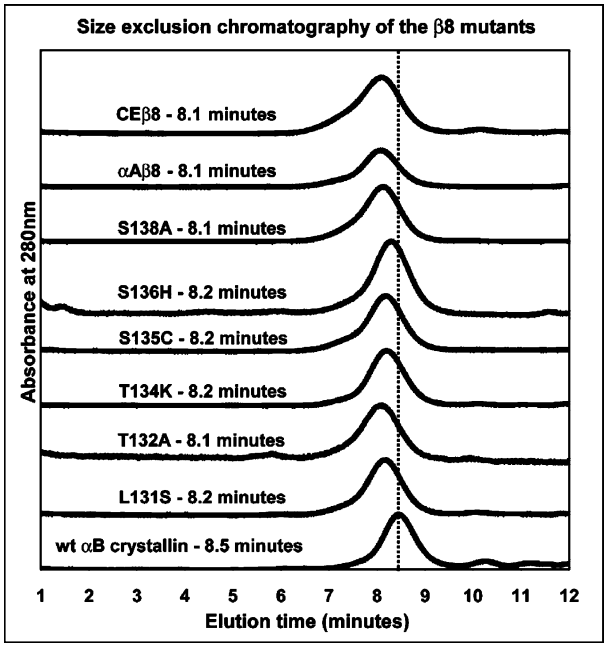

FIGURE 5: Size exclusion chromatography of wt αB crystallin and the eight β8 mutants. Elution profiles of wt αB crystallin and the eight β8 mutants were recorded on a HPLC Biosep SEC-S4000 column with a molecular mass range of 15−2000 kDa. Wt αB crystallin eluted at 8.5 min corresponding to an apparent mean molecular mass of 472 kDa or 23 subunits per assembly. The elution times of the six single-site β8 mutants, L131S (8.2 min), T132A (8.1 min), T134K (8.2 min), S135C (8.2 min), S136H (8.2 min), and S138A (8.1 min), and both chimeric β8 mutants, αAβ8 (8.1 min) and CEβ8 (8.1 min), were shorter than wt αB crystallin, indicating that mutations in the β8 motif altered the complex size of αB crystallin.

far-UVCD spectra of the β8 mutants at both 37 and 50 °C were similar to wt αB crystallin, which demonstrated the similarity in structure and thermal stability of the β8 mutants and wt αB crystallin.

The effects of the β8 mutations on the complex assembly of αB crystallin were measured using size exclusion chromatography (Figure 5). The elution times of all six single-site β8 mutants were 8.1−8.2 min, which was shorter than the elution time of 8.5 min measured for wt αB crystallin. The difference in elution time corresponded to an increase of 6−8 subunits/assembly in the complex size of αB crystallin (Table 2). Similarly, both multisite chimeric β8 mutants, αAβ8 and CEβ8, had shorter elution times (8.1 min) which corresponded to an increase in complex size by approximately 8 subunits/assembly relative to wt αB crystallin. Size exclusion chromatography of the single-site and chimeric β8 mutants was consistent with the involvement of the β8 interactive sequence in the complex assembly of αB crystallin subunits.

The chaperone activities of wt αB crystallin and the eight β8 mutants were assessed in vitro using thermal aggregation assays with three substrates, β_L crystallin, a physiological chaperone substrate protein (Figure 6A), and two model chaperone substrate proteins, ADH (Figure 6B) and CS (Figure 6C). The three substrates were selected for the chaperone assays to determine the substrate selectivity of specific residues of the β8 interactive sequence because they have different unfolding and aggregation characteristics (*25*). The amount of unfolding and aggregation of the substrates was CS $\gg$ ADH $>$ β_L crystallin (*25*, *27*). The single-site β8 mutants, L131S, T132A, and S135C, had chaperone activity comparable to wt αB crystallin with the target proteins β_L crystallin and ADH (Table 3). In contrast, the single-site β8 mutants T134K, S136H, and S138A reduced or lost chaperone activity with the target proteins β_L crystallin and ADH. The T134K mutant had no chaperone activity with CS, and the remaining five single-site β8 mutants had ~45−66% of the chaperone activity measured for wt αB crystallin with CS. The αAβ8 and CEβ8 chimeric mutants had lower chaperone activity relative to wt αB crystallin with all three substrate proteins. Mutating residues Leu-131, Thr-132, and Ser-135 had a larger effect on the aggregation of CS than on the aggregation of β_L crystallin and ADH. In contrast, mutating residues Thr-134, Ser-136, and Ser-138 had a larger effect on the aggregation of β_L crystallin and ADH than on the aggregation of CS.

The exposed, nonconserved residues of the β8 sequence, $_{131}$**LT**I**TSS**L**S**$_{138}$, were mapped to the surface of the α crystallin core domain in a space-filled model of human αB crystallin (Figure 7). In the model, the β4 and β8 strands form a groove of hydrophilic and hydrophobic interactive sites on the external surface of the α crystallin core domain (purple). Complex assembly may involve interactions between the Ile-Pro-Ile (I-X-I) motif of the C-terminal extension of one αB crystallin (tan ribbon) and the β4−β8 groove (purple) of another subunit similar to the complex assembly of *Methanococcus jannaschii* sHSP16.5 and wheat sHSP16.9. In addition, the β8 strand contributes residues, Leu-131, Thr-132, Thr-134, Ser-136, and Ser-138 to form the β3−β8−β9

Table 2: Complex Size of wt αB Crystallin and the Eight β8 Mutants[a]

protein	molecular mass of subunit (kDa)	elution time (min)	polydispersity (min)	apparent molecular mass (kDa)	no. of subunits/ assembly
wt αB crystallin	20.2	8.5	0.7	472 ± 22	23 ± 1
L131S	20.1	8.2	0.8	577 ± 12	29 ± 1
T132A	20.1	8.1	0.9	617 ± 8	31 ± 0
T134K	20.2	8.2	0.8	577 ± 15	29 ± 1
S135C	20.2	8.2	0.8	577 ± 5	29 ± 0
S136H	20.2	8.2	0.8	577 ± 54	29 ± 3
S138A	20.1	8.1	0.8	617 ± 5	31 ± 0
αAβ8	20.1	8.1	0.8	617 ± 16	31 ± 1
CEβ8	20.2	8.1	1.0	617 ± 20	31 ± 1

[a] Column 1 lists the protein. Column 2 lists the molecular mass of an αB crystallin (wt or mutant) subunit calculated from its primary sequence. Column 3 lists the average measured elution time from three separate chromatographs. Column 4 lists the average polydispersity of the elution peaks, which was defined as the width of the elution peak at half peak height. Column 5 lists the apparent molecular mass calculated from the elution time. Column 6 lists the average number of subunits per assembly calculated from the apparent molecular mass.

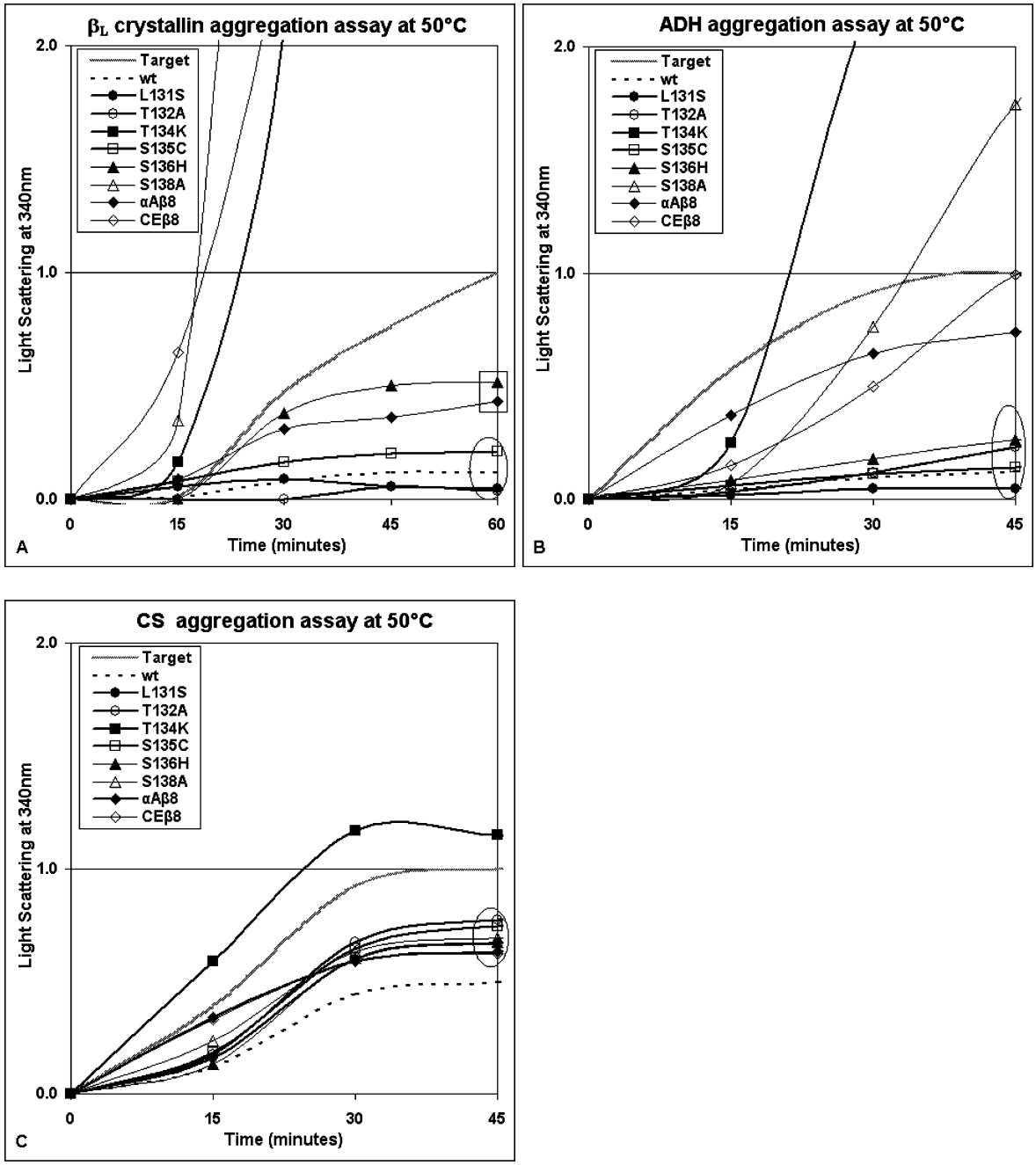

FIGURE 6: Chaperone activity of wt αB crystallin and the eight β8 mutants. The effects of wt αB crystallin and the β8 mutants on the thermal aggregation of β_L crystallin (A), ADH (B), and CS (C) at 1:1 monomeric molar ratio were measured as light scattering at $\lambda = 340$ nm using a spectrophotometer. (A) The effects of L131S, T132A, and S135C were comparable to wt αB crystallin in the aggregation of β_L crystallin (enclosed in the oval). S136H and αAβ8 were less effective than wt αB crystallin on the aggregation of β_L crystallin (enclosed in the square). T134K, S138A, and CEβ8 were ineffective, increasing the aggregation of β_L crystallin more than 50-fold (off scale). (B) The effects of L131S, T132A, S135C, and S136H were comparable to wt αB crystallin on the aggregation of ADH (enclosed in the oval). T134K, S138A, αAβ8, and CEβ8 were ineffective chaperones, and the aggregation of ADH increased more than 6-fold relative to wt αB crystallin. (C) L131S, T132A, S135C, S136H, S138A, αAβ8, and CEβ8 had a modest effect on the aggregation of CS (enclosed in the oval). T134K was the least effective on the aggregation of CS. Overall, the chaperone activity toward β_L crystallin and ADH was decreased by mutations at three of the six residues in the β8 motif of αB crystallin, and the chaperone activity toward CS was decreased by mutations to all six residues in the β8 motif of αB crystallin.

chaperone interface on the surface of the α crystallin core domain.

DISCUSSION

In this report, residues in the β8 sequence, $_{131}$**LTITSSLS**$_{138}$, were mutated to evaluate their effect on the complex assembly and chaperone activity of human αB crystallin. The similarities in UVCD spectra of the β8 mutants demonstrated that substitution of the nonconserved, surface-exposed residues of the β8 motif had minimal effect on the β sheet structure of the α crystallin core domain. Size exclusion chromatography of the β8 mutants determined that mutating residues Leu-131, Thr-132, Thr-134, Ser-135, Ser-136, and Ser-138 increased the complex size of αB crystallin

Table 3: Summarized Results for Chaperone Activity of wt αB Crystallin and the Eight β8 Mutants[a]

	β_L crystallin		alcohol dehydrogenase (ADH)		citrate synthase (CS)	
chaperone	aggregation	chaperone activity (%)	aggregation	chaperone activity (%)	aggregation	chaperone activity (%)
wt αB crystallin	0.12 ± 0.06	100	0.12 ± 0.00	100	0.50 ± 0.01	100
L131S	0.05 ± 0.05	108	0.05 ± 0.01	109	0.67 ± 0.08	66
T132A	0.04 ± 0.05	109	0.23 ± 0.03	88	0.77 ± 0.05	45
T134K	12.50 ± 1.53	0	2.92 ± 0.14	0	1.15 ± 0.07	0
S135C	0.21 ± 0.11	90	0.14 ± 0.01	98	0.74 ± 0.12	51
S136H	0.52 ± 0.09	55	0.26 ± 0.03	84	0.67 ± 0.06	65
S138A	14.09 ± 1.72	0	1.75 ± 0.17	0	0.69 ± 0.10	61
αAβ8	0.43 ± 0.04	64	0.74 ± 0.01	30	0.16 ± 0.04	73
CEβ8	6.09 ± 0.38	0	0.99 ± 0.01	1	0.62 ± 0.13	75

[a] Column 1 lists the chaperone. Columns 2, 4, and 6 list the normalized aggregation of the substrates, β_L crystallin, ADH, and CS, respectively, in the absence or presence of a chaperone. Columns 3, 5, and 7 list the chaperone activity of the chaperones as percent protection. The aggregation of the substrates after heating to 50 °C for 60 min in the absence of a chaperone corresponded to 0% protection, and the chaperone activity of wt αB crystallin corresponded to 100% protection. Chaperone activities calculated from aggregation values that were higher than the aggregation values of the substrates in the absence of any chaperone were set to 0% protection.

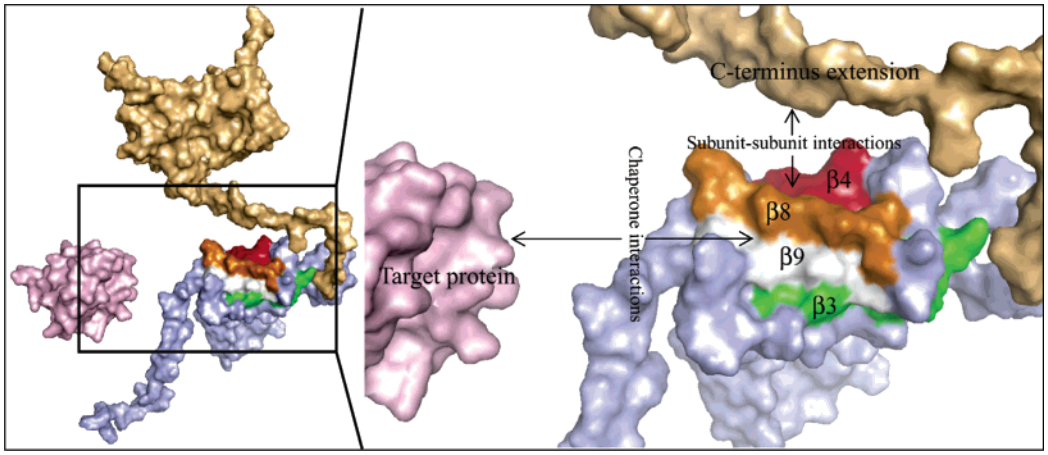

FIGURE 7: 3-D computer model for the β3−β8−β9 interface on the surface of the α crystallin core domain of human αB crystallin. In the space-filled model of human αB crystallin (purple), the exposed side chains of the β3−β8-β9 interface are shown as green (β3), orange (β8), and white (β9) surfaces. The exposed side chains of the β4 strand are in red. Complex assembly is the result of subunit−subunit interactions that involves an interaction of the C-terminal extension of one αB crystallin molecule (tan) with the β4−β8 interface on the surface of the α crystallin core domain of a second αB crystallin molecule (purple). Chaperone activity is the result of interactions between the β3−β8−β9 interface on the surface of αB crystallin (purple) and the exposed residues of an unfolding target substrate protein (pink). The exposed residues, Asn-78, Lys-82, and His-83 of the β3 sequence, Leu-131, Thr-132, Thr-134, Ser-136, and Ser-138 of the β8 sequence, and Gly-141 and Thr-144 of the β9 sequence together form the β3−β8−β9 chaperone interface on the surface of the α crystallin core domain.

by six to eight subunits (*24*). The mutational analysis confirmed the results of the pin array analysis which identified the β8 sequence as an interactive domain in both αA and αB crystallin (*24*). The results were consistent with the X-ray crystal structures of *M. jannaschii* sHSP16.5 and wheat sHSP16.9, in which the residues of the C-terminal Ile-X-Ile/Val motif of one subunit interacted with residues of the β4−β8 groove of another subunit to form complexes (*20*, *21*). The results established the β8 sequence of αB crystallin as an important sequence for subunit−subunit interactions that result in complex assembly.

The effects of substituting residues in the β8 motif of αB crystallin with homologous residues from the β8 motif of *C. elegans* sHSP12.2, a sHSP that lacks chaperone activity in vitro, were dramatic. The *C. elegans* sHSP12.2 based β8 mutants, T134K, S136H, S138A, and CEβ8, had diminished chaperone activities relative to wt αB crystallin for all three substrates. Substituting residues in the β8 motif of αB crystallin with homologous residues from the β8 motif of αA crystallin had no effect on chaperone activity for substrate proteins β_L crystallin and ADH and diminished chaperone activity for the substrate protein CS. One interpretation of these results is that residues Thr-134, Ser-136, and Ser-138 of the β8 motif that occupy prominent locations on the surface of the α crystallin core domain are critical for overall chaperone activity independent of the amount of substrate protein unfolding. Residues Leu-131, Thr-132, and Ser-135 of the β8 motif are important for substrate interactions and may recognize and preferentially select completely unfolded substrates such as CS for chaperone activity. The results presented in this report are consistent with the hypothesis that the surface-exposed residues of the β8 motif (Thr-134, Ser-136, and Ser-138) combined with the surface-exposed residues of the β3 motif (Asn-78, Lys-82, and His-83) (*27*) and the β9 motif (Gly-141 and Thr-144) (*19*) form an interface for chaperone activity in αB crystallin (Figure 7). The effect of mutations in the β8 motif on chaperone activity can be attributed to local changes in the surface resulting from substitutions of the nonconserved, exposed residues of the β8 sequence. We note that the 3-D structure of the conserved α crystallin core domain of human αB crystallin is an immunoglobulin-like fold consisting of seven β strands

arranged in an antiparallel orientation to form a compact β sandwich. β strands 2, 3, 8, and 9 form one β sheet, while β strands 4, 5, and 7 form the antiparallel β sheet. Residues Leu-131, Thr-132, Thr-136, Ser136, and Ser138 are involved in formation of the β3−β8−β9 chaperone interface (Figure 7, orange, white, and green surfaces), and residues Leu-131, Ser-135, and Leu-137 are involved in formation of the shallow β4−β8 groove on the surface of the α crystallin core domain (Figure 7, orange and red surfaces) for subunit−subunit interactions (*19*−*21*, *24*, *25*). The β8 strand contributes residues to each of the two separate interfaces (Figure 7).

While the effect of the β8 mutations on chaperone activity was variable, the effect on assembly of multimeric complexes was consistent in that the complexes formed by all eight β8 mutants were larger than wt αB crystallin by 6−8 subunits. The findings demonstrated that the chaperone activity of αB crystallin was independent of complex size. Assemblies of αB crystallin are polydisperse and dynamic, suggesting that altered complex ↔ subunit exchange may modify the chaperone activity of the β8 mutants in the absence of an effect on complex size. In the assembled complex, the surface-exposed interactive residues of the β3−β8−β9 interface of the assembled αB crystallin subunits may be buried in the oligomer and inaccessible to unfolding proteins, leading to the hypothesis that dissociation of αB crystallin complexes is required for effective chaperone activity. This hypothesis is supported by recent studies in which dissociation of sHSP oligomers was observed to regulate the chaperone activity of sHSPs (*42*−*56*). The absence of a correlation between complex size and chaperone activity suggested that the polydispersity resulting from a dynamic subunit exchange rate may be more important than complex size in regulating the chaperone activity of sHSPs (*43*, *53*, *57*−*61*). This hypothesis is under investigation in separate studies.

In summary, the results confirmed the importance of the nonconserved, surface-exposed residues of the β8 sequence for subunit−subunit interactions in complex assembly and in interactions with unfolding proteins during chaperone activity.

REFERENCES

1. Srinivasan, A. N., Nagineni, C. N., and Bhat, S. P. (1992) alpha A-crystallin is expressed in nonocular tissues, *J. Biol. Chem. 267*, 23337−23341.
2. Iwaki, T., Iwaki, A., Miyazono, M., and Goldman, J. E. (1991) Preferential expression of alpha B-crystallin in astrocytic elements of neuroectodermal tumors, *Cancer 68*, 2230−2240.
3. Iwaki, T., Iwaki, A., Liem, R. K., and Goldman, J. E. (1991) Expression of alpha B-crystallin in the developing rat kidney, *Kidney Int. 40*, 52−56.
4. Iwaki, T., Kume-Iwaki, A., and Goldman, J. E. (1990) Cellular distribution of alpha B-crystallin in nonlenticular tissues, *J. Histochem. Cytochem. 38*, 31−39.
5. Iwaki, T., Kume-Iwaki, A., Liem, R. K., and Goldman, J. E. (1989) Alpha B-crystallin is expressed in non-lenticular tissues and accumulates in Alexander's disease brain, *Cell 57*, 71−78.
6. Atomi, Y., Yamada, S., Strohman, R., and Nonomura, Y. (1991) Alpha B-crystallin in skeletal muscle: purification and localization, *J. Biochem. (Tokyo) 110*, 812−822.
7. Bhat, S. P., Horwitz, J., Srinivasan, A., and Ding, L. (1991) Alpha B-crystallin exists as an independent protein in the heart and in the lens, *Eur. J. Biochem. 202*, 775−781.
8. Lowe, J., Landon, M., Pike, I., Spendlove, I., McDermott, H., and Mayer, R. J. (1990) Dementia with beta-amyloid deposition: involvement of alpha B-crystallin supports two main diseases, *Lancet 336*, 515−516.
9. Zantema, A., Verlaan-De Vries, M., Maasdam, D., Bol, S., and van der Eb, A. (1992) Heat shock protein 27 and alpha B-crystallin can form a complex, which dissociates by heat shock, *J. Biol. Chem. 267*, 12936−12941.
10. Carver, J. A., Aquilina, J. A., Cooper, P. G., Williams, G. A., and Truscott, R. J. (1994) Alpha-crystallin: molecular chaperone and protein surfactant, *Biochim. Biophys. Acta 1204*, 195−206.
11. Rao, P. V., Horwitz, J., and Zigler, J. S., Jr. (1993) Alpha-crystallin, a molecular chaperone, forms a stable complex with carbonic anhydrase upon heat denaturation, *Biochem. Biophys. Res. Commun. 190*, 786−793.
12. Horwitz, J. (1992) Alpha-crystallin can function as a molecular chaperone, *Proc. Natl. Acad. Sci. U.S.A. 89*, 10449−10453.
13. Arrigo, A. P. (1998) Small stress proteins: chaperones that act as regulators of intracellular redox state and programmed cell death, *Biol. Chem. 379*, 19−26.
14. Narberhaus, F. (2002) Alpha-crystallin-type heat shock proteins: socializing minichaperones in the context of a multichaperone network, *Microbiol. Mol. Biol. Rev. 66*, 64−93 (table of contents).
15. Guruprasad, K., and Kumari, K. (2003) Three-dimensional models corresponding to the C-terminal domain of human alphaA- and alphaB-crystallins based on the crystal structure of the small heat-shock protein HSP16.9 from wheat, *Int. J. Biol. Macromol. 33*, 107−112.
16. Valdez, M. M., Clark, J. I., Wu, G. J., and Muchowski, P. J. (2002) Functional similarities between the small heat shock proteins *Mycobacterium tuberculosis* HSP 16.3 and human alphaB-crystallin, *Eur. J. Biochem. 269*, 1806−1813.
17. Koteiche, H. A., and McHaourab, H. S. (1999) Folding pattern of the alpha-crystallin domain in alphaA-crystallin determined by site-directed spin labeling, *J. Mol. Biol. 294*, 561−577.
18. Muchowski, P. J., Hays, L. G., Yates, J. R., III, and Clark, J. I. (1999) ATP and the core "alpha-crystallin" domain of the small heat-shock protein alphaB-crystallin, *J. Biol. Chem. 274*, 30190−30195.
19. Muchowski, P. J., Wu, G. J., Liang, J. J., Adman, E. T., and Clark, J. I. (1999) Site-directed mutations within the core "alpha-crystallin" domain of the small heat-shock protein, human alphaB-crystallin, decrease molecular chaperone functions, *J. Mol. Biol. 289*, 397−411.
20. Kim, K. K., Kim, R., and Kim, S. H. (1998) Crystal structure of a small heat-shock protein, *Nature 394*, 595−599.
21. van Montfort, R. L., Basha, E., Friedrich, K. L., Slingsby, C., and Vierling, E. (2001) Crystal structure and assembly of a eukaryotic small heat shock protein, *Nat. Struct. Biol. 8*, 1025−1030.
22. Crabbe, M. J., and Goode, D. (1995) Protein folds and functional similarity; the Greek key/immunoglobulin fold, *Comput. Chem. 19*, 343−349.
23. Stamler, R., Kappe, G., Boelens, W., and Slingsby, C. (2005) Wrapping the alpha-crystallin domain fold in a chaperone assembly, *J. Mol. Biol. 353*, 68−79.
24. Ghosh, J. G., and Clark, J. I. (2005) Insights into the domains required for dimerization and assembly of human alphaB crystallin, *Protein Sci. 14*, 684−695.
25. Ghosh, J. G., Estrada, M. R., and Clark, J. I. (2005) Interactive domains for chaperone activity in the small heat shock protein, human alphaB crystallin, *Biochemistry 44*, 14854−14869.
26. Koteiche, H. A., Berengian, A. R., and McHaourab, H. S. (1998) Identification of protein folding patterns using site-directed spin labeling. Structural characterization of a beta-sheet and putative substrate binding regions in the conserved domain of alpha A-crystallin, *Biochemistry 37*, 12681−12688.
27. Ghosh, J. G., Estrada, M. S., and Clark, J. I. (2006) The function of the β3 interactive domain in the small heat shock protein and molecular chaperone, human αB crystallin, *Cell Stress Chaperones 11*, 187−197.
28. Feil, I. K., Malfois, M., Hendle, J., van Der Zandt, H., and Svergun, D. I. (2001) A novel quaternary structure of the dimeric alpha-crystallin domain with chaperone-like activity, *J. Biol. Chem. 276*, 12024−12029.
29. Derham, B. K., van Boekel, M. A., Muchowski, P. J., Clark, J. I., Horwitz, J., Hepburne-Scott, H. W., de Jong, W. W., Crabbe, M. J., and Harding, J. J. (2001) Chaperone function of mutant versions of alpha A- and alpha B-crystallin prepared to pinpoint chaperone binding sites, *Eur. J. Biochem. 268*, 713−721.
30. Bera, S., Thampi, P., Cho, W. J., and Abraham, E. C. (2002) A positive charge preservation at position 116 of alpha A-crystallin

is critical for its structural and functional integrity, *Biochemistry 41*, 12421−12426.
31. Cherian, M., and Abraham, E. C. (1995) Decreased molecular chaperone property of alpha-crystallins due to posttranslational modifications, *Biochem. Biophys. Res. Commun. 208*, 675−679.
32. Shroff, N. P., Bera, S., Cherian-Shaw, M., and Abraham, E. C. (2001) Substituted hydrophobic and hydrophilic residues at methionine-68 influence the chaperone-like function of alphaB-crystallin, *Mol. Cell. Biochem. 220*, 127−133.
33. Sreelakshmi, Y., Santhoshkumar, P., Bhattacharyya, J., and Sharma, K. K. (2004) alphaA-crystallin interacting regions in the small heat shock protein, alphaB-crystallin, *Biochemistry 43*, 15785−15795.
34. Bhattacharyya, J., and Sharma, K. K. (2001) Conformational specificity of mini-alphaA-crystallin as a molecular chaperone, *J. Pept. Res. 57*, 428−434.
35. Sharma, K. K., Kaur, H., and Kester, K. (1997) Functional elements in molecular chaperone alpha-crystallin: identification of binding sites in alpha B-crystallin, *Biochem. Biophys. Res. Commun. 239*, 217−222.
36. Sharma, K. K., Kumar, G. S., Murphy, A. S., and Kester, K. (1998) Identification of 1,1′-bi(4-anilino)naphthalene-5,5′-disulfonic acid binding sequences in alpha-crystallin, *J. Biol. Chem. 273*, 15474−15478.
37. Sharma, K. K., Kaur, H., Kumar, G. S., and Kester, K. (1998) Interaction of 1,1′-bi(4-anilino)naphthalene-5,5′-disulfonic acid with alpha-crystallin, *J. Biol. Chem. 273*, 8965−8970.
38. Sreelakshmi, Y., and Sharma, K. K. (2001) Interaction of alpha-lactalbumin with mini-alphaA-crystallin, *J. Protein Chem. 20*, 123−130.
39. Santhoshkumar, P., and Sharma, K. K. (2001) Phe71 is essential for chaperone-like function in alpha A-crystallin, *J. Biol. Chem. 276*, 47094−47099.
40. Kokke, B. P., Leroux, M. R., Candido, E. P., Boelens, W. C., and de Jong, W. W. (1998) *Caenorhabditis elegans* small heat-shock proteins Hsp12.2 and Hsp12.3 form tetramers and have no chaperone-like activity, *FEBS Lett. 433*, 228−232.
41. Kokke, B. P., Boelens, W. C., and de Jong, W. W. (2001) The lack of chaperonelike activity of *Caenorhabditis elegans* Hsp12.2 cannot be restored by domain swapping with human alphaB-crystallin, *Cell Stress Chaperones 6*, 360−367.
42. Srinivas, V., Raman, B., Rao, K. S., Ramakrishna, T., and Rao Ch, M. (2005) Arginine hydrochloride enhances the dynamics of subunit assembly and the chaperone-like activity of alpha-crystallin, *Mol. Vision 11*, 249−255.
43. Shashidharamurthy, R., Koteiche, H. A., Dong, J., and McHaourab, H. S. (2005) Mechanism of chaperone function in small heat shock proteins: dissociation of the HSP27 oligomer is required for recognition and binding of destabilized T4 lysozyme, *J. Biol. Chem. 280*, 5281−5289.
44. Zhang, H., Fu, X., Jiao, W., Zhang, X., Liu, C., and Chang, Z. (2005) The association of small heat shock protein Hsp16.3 with the plasma membrane of *Mycobacterium tuberculosis*: dissociation of oligomers is a prerequisite, *Biochem. Biophys. Res. Commun. 330*, 1055−1061.
45. Fu, X., Zhang, H., Zhang, X., Cao, Y., Jiao, W., Liu, C., Song, Y., Abulimiti, A., and Chang, Z. (2005) A dual role for the N-terminal region of *Mycobacterium tuberculosis* Hsp16.3 in self-oligomerization and binding denaturing substrate proteins, *J. Biol. Chem. 280*, 6337−6348.
46. Stromer, T., Fischer, E., Richter, K., Haslbeck, M., and Buchner, J. (2004) Analysis of the regulation of the molecular chaperone Hsp26 by temperature-induced dissociation: the N-terminal domail is important for oligomer assembly and the binding of unfolding proteins, *J. Biol. Chem. 279*, 11222−11228.
47. Haslbeck, M., Ignatiou, A., Saibil, H., Helmich, S., Frenzl, E., Stromer, T., and Buchner, J. (2004) A domain in the N-terminal part of Hsp26 is essential for chaperone function and oligomerization, *J. Mol. Biol. 343*, 445−455.
48. Fu, X., Jiao, W., Abulimiti, A., and Chang, Z. (2004) Inter-subunit cross-linking suppressed the dynamic oligomeric dissociation of *Mycobacterium tuberculosis* Hsp16.3 and reduced its chaperone activity, *Biochemistry (Moscow) 69*, 552−557.
49. Lentze, N., Aquilina, J. A., Lindbauer, M., Robinson, C. V., and Narberhaus, F. (2004) Temperature and concentration-controlled dynamics of rhizobial small heat shock proteins, *Eur. J. Biochem. 271*, 2494−2503.
50. Fu, X., and Chang, Z. (2004) Temperature-dependent subunit exchange and chaperone-like activities of Hsp16.3, a small heat shock protein from *Mycobacterium tuberculosis*, *Biochem. Biophys. Res. Commun. 316*, 291−299.
51. Fu, X., Liu, C., Liu, Y., Feng, X., Gu, L., Chen, X., and Chang, Z. (2003) Small heat shock protein Hsp16.3 modulates its chaperone activity by adjusting the rate of oligomeric dissociation, *Biochem. Biophys. Res. Commun. 310*, 412−420.
52. Gu, L., Abulimiti, A., Li, W., and Chang, Z. (2002) Monodisperse Hsp16.3 nonamer exhibits dynamic dissociation and reassociation, with the nonamer dissociation prerequisite for chaperone-like activity, *J. Mol. Biol. 319*, 517−526.
53. Liu, L., Ghosh, J. G., Clark, J. I., and Jiang, S. (2006) Studies of alphaB crystallin subunit dynamics by surface plasmon resonance, *Anal. Biochem 350*, 186−195.
54. Spinozzi, F., Mariani, P., Rustichelli, F., Amenitsch, H., Bennardini, F., Mura, G. M., Coi, A., and Ganadu, M. L. (2006) Temperature dependence of chaperone-like activity and oligomeric state of alphaB-crystallin, *Biochim. Biophys. Acta* (in press).
55. Skouri-Panet, F., Quevillon-Cheruel, S., Michiel, M., Tardieu, A., and Finet, S. (2006) sHSPs under temperature and pressure: The opposite behaviour of lens alpha-crystallins and yeast HSP26, *Biochim. Biophys. Acta* (in press).
56. Koteiche, H. A., and McHaourab, H. S. (2006) Mechanism of a hereditary cataract phenotype: mutations in alpha A-crystallin activate substrate binding, *J. Biol. Chem.* (in press).
57. Giese, K. C., and Vierling, E. (2002) Changes in oligomerization are essential for the chaperone activity of a small heat shock protein in vivo and in vitro, *J. Biol. Chem. 277*, 46310−46318.
58. Yang, H., Huang, S., Dai, H., Gong, Y., Zheng, C., and Chang, Z. (1999) The *Mycobacterium tuberculosis* small heat shock protein Hsp16.3 exposes hydrophobic surfaces at mild conditions: conformational flexibility and molecular chaperone activity, *Protein Sci. 8*, 174−179.
59. Datta, S. A., and Rao, C. M. (2000) Packing-induced conformational and functional changes in the subunits of alpha-crystallin, *J. Biol. Chem. 275*, 41004−41010.
60. Lindner, R. A., Kapur, A., Mariani, M., Titmuss, S. J., and Carver, J. A. (1998) Structural alterations of alpha-crystallin during its chaperone action, *Eur. J. Biochem. 258*, 170−183.
61. McHaourab, H. S., Dodson, E. K., and Koteiche, H. A. (2002) Mechanism of chaperone function in small heat shock proteins. Two-mode binding of the excited states of T4 lysozyme mutants by alphaA-crystallin, *J. Biol. Chem. 277*, 40557−40566.

BI060970K